System Design of Fast Actuator for Vacuum Interrupter in DC Applications

Tim Augustin
KTH Royal Institute of Technology
Stockholm, Sweden
timau@kth.se

Jesper Magnusson
ABB Corporate Research Center
Västerås, Sweden

Mrunal Parekh
KTH Royal Institute of Technology
Stockholm, Sweden

Marley Becerra Garcia
KTH Royal Institute of Technology
Stockholm, Sweden

Hans-Peter Nee
KTH Royal Institute of Technology
Stockholm, Sweden

***Abstract*—One of the major challenges of DC circuit breakers is the required fast mechanical actuator. In this paper, a Thomson coil actuator system for a vacuum interrupter is designed. Active damping is used to decelerate the moving contacts. Challenges are discussed, especially concerning the power supply needed for the Thomson coil actuator. The design philosophy is explained and FEM simulation results are presented. The results indicate that a wide range of combinations of drive circuit capacitance and voltage fulfill the requirements for armature acceleration. However, active damping requires a very careful selection of drive circuit voltage and timing of applied damping.**

***Keywords*—DC circuit breaker, vacuum interrupter, Thomson coil actuator, fast mechanical switch, active damping**

I. INTRODUCTION

DC circuit breakers (DCCBs) are subject to intense on-going research activities due to the prospect of DC grids. DCCBs are expected to open fast with interruption times of a few milliseconds. Numerous DCCB topologies have been proposed, which can broadly be categorized as current injection DCCBs and hybrid DCCBs, see [1], [2] for an overview. In current injection DCCBs, the arc in a mechanical switch is interrupted by injecting a current to cause a local current zero. In hybrid DCCBs, mechanical switches are combined with power electronics to interrupt current. Both DCCB types require a mechanical switch. Vacuum interrupters (VIs) are an option as mechanical switch because the moving parts are relatively light and the $\mathrm{d}i/\mathrm{d}t$ interruption capability at current zero is superior compared to gas circuit breakers [3]. In order to open VIs at the required speed, conventional spring or electromagnetic actuators are not sufficient. Thomson coil actuators (TCAs) allow for very fast opening [4]. As the contact gap of VIs is relatively short[1], it is difficult to both accelerate and decelerate the moving contact leading to contact bouncing or unintentional reclosing. A potential solution is active damping [5], [6].

In this work, the system design for a TCA for a VI with active damping is explained. In contrast to previous work, practical challenges such as the requirements posed on the power supply by auto-reclosing and proactive commutation operation are discussed. The TCA is going to be used with an embedded pole VI to test DCCB concepts in an advanced test circuit that is currently under construction [7]. In Section II, system aspects regarding the DCCB, its actuator system, and design methodology are described. In Section III, FEM modelling of the TCA is explained. In Section IV, simulation results are presented for opening and closing operation. In Section V, all findings are summarized.

[1] $10\,\mathrm{mm}$ for the $12\,\mathrm{kV}$ VI used in this work

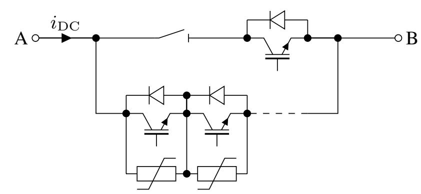

Fig. 1. ABB's hybrid DC circuit breaker

II. SYSTEM DESCRIPTION

A. Hybrid DC Circuit Breaker

Hybrid DCCBs combine power electronics and mechanical switches to interrupt DC. Many different concepts have been proposed which nevertheless perform similarly. Therefore, only ABB's concept shown in Fig. 1 is covered as example. The main path consisting of an ultra-fast disconnector (UFD) and a load commutation switch (LCS) conducts in normal operation. The LCS is an IGBT stack with only a few series-connected IGBT positions. The commutation path is made up by several IGBT stacks, each consisting of many series-connected IGBTs. When the internal DCCB logic detects a potential fault, the LCS is turned off and the switches in the commutation path are turned on to commutate the current into this path proactively. The UFD is opened and after $2\,\mathrm{ms}$ it has sufficient dielectric withstand capability. If the protection system trips the DCCB unit, the current is commutated into the metal-oxide varistors of the energy absorption path by turning off the IGBTs in the commutation path which forces

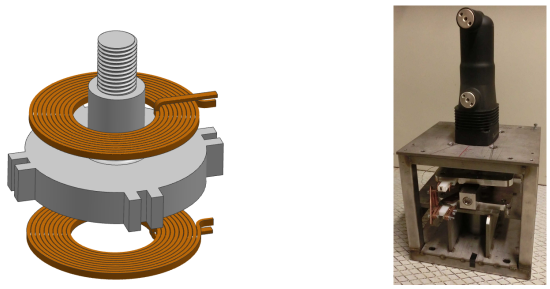

(a) CAD illustration (b) Prototype

Fig. 2. Thomson coil actuator system for vacuum interrupter

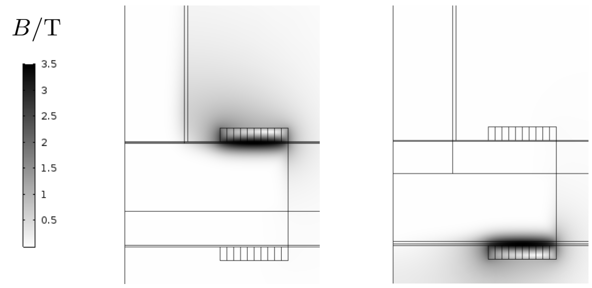

(a) Acceleration (b) Damping

Fig. 3. Magnetic flux density during opening operation

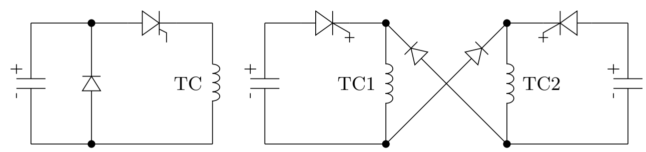

(a) Conventional (b) Combined for opening and closing

Fig. 4. Drive circuits for Thomson coil actuator

the current to zero. However, a recent study [8] has shown that the conduction time of the semiconductors in the commutation path has to be limited to $5\,\mathrm{ms}$ depending on the utilized semiconductor technology. If the DCCB unit has not been tripped after a defined time and the internal DCCB logic evaluates the circumstances as non-critical, the current is commutated back to the main path by firstly closing the UFD and then turning on the LCS.

Potentially, a VI could be used instead of a UFD in the main path. This would be beneficial due to the low moving contact mass of VIs and the fact that SF6 is avoided. Furthermore, if a component fails, arcing would not be a problem in contrast to a UFD which is not designed for arcing. An LCS is needed as the arc voltage of a VI is too low for commutation [9]. In overhead line systems, DCCBs have to be able to auto-reclose. Typical deionization times in the range of a few hundred milliseconds and aborting of proactive commutation after $5\,\mathrm{ms}$ pose challenging constraints on the TCA and its power supply.

B. Thomson Coil Actuator

Two Thomson coils (TCs) as shown in Fig. 2a are used - one for opening and one for closing. The TC has to be excited with a pulse current for operation. This pulse induces eddy currents in the armature which causes a repelling magnetic field. An off-the-shelf VI in an embedded pole is used with a TCA, see Fig. 2b. The embedded pole includes all required mechanical components apart from the TCA.

C. Active Damping

For active damping, one TC is excited to accelerate the armature and the other TC to decelerate the armature. For instance, the opening TC is excited to open and shortly before the VI is fully opened, the closing TC is excited and vice-versa for closing. The principle is shown in Fig. 3.

D. Drive Circuit

The TC is excited by discharging a capacitor. This can be done with a conventional drive circuit as shown in Fig. 4a. Separate drive circuits are used for each TC. This implies that both capacitors are discharged after opening or closing, respectively. If the contacts have to be reclosed or reopened, for instance after $5\,\mathrm{ms}$ due to an aborted proactive commutation, the capacitors have to be charged fast. A solution could be adding backup capacitors or a powerful power supply. As alternative, the drive circuits of both TCs could be combined into one drive circuit which uses the stored energy in one TC for damping in the other TC. An example is shown in Fig. 4b. To start damping, one of the IGCTs is turned off. The current starts to freewheel through the other TC causing a damping effect. We did not succeed to get sufficient damping from this configuration in simulations, but it cannot be excluded that in TCAs with other requirements it may work. Hence, two separate conventional drive circuits are used in this study.

E. Power Supply

Three common methods for capacitor bank charging are resistive charging, resonant charging, and constant current charging. Resistive charging means that the capacitor is connected to a resistor and a power source to charge up. The charging time is determined by the RC time constant and is inherently slow. Resonant charging means that the capacitor bank to be charged is connected to a supply capacitor bank via a switch and an inductor. By closing the switch the supply capacitor bank discharges into the other capacitor bank, thus charging it up. The advantage is that the charging time is determined by the resonant period of the LC circuit which is typically much shorter than an RC time constant. Constant current charging refers to a method where a switch-mode power supply is used to provide the charging current. Switch-mode power supplies are relatively compact. The bottleneck is that with e.g. a $45\,\mathrm{kW}$ power supply charging a $10\,\mathrm{mF}$ capacitor up to $500\,\mathrm{V}$ takes $55.6\,\mathrm{ms}$. Considering typical deionization times, this would be sufficient for a simple active resonant DCCB. If proactive commutation is to be utilized, a solution with one capacitor per Thomson coil would require recharging within $5\,\mathrm{ms}$ which would require a more powerful power supply. If one capacitor is used for opening and closing acceleration and damping, respectively, the capacitors would still be completely discharged after an aborted proactive commutation and the closed DCCB would be inoperable until the capacitors are recharged. Hence, a resonant charging circuit could be preferable in this case.

F. Design Rules

To determine feasible combinations of the voltage U and capacitance C of the drive circuit, a parameter study has been performed. This study was performed for opening as the bellows exerts an opposing force on the armature during opening, but during closing it aids. Fast operation time is not the only requirement. Keeping the power supply challenge in mind, U and C should be chosen according to the chosen power supply, for instance for minimum energy or minimum C. The goal is that the armature reaches a peak velocity of $3\,\mathrm{m\,s^{-1}}$. Therefore, a tolerance band of $2.5\,\mathrm{m\,s^{-1}}$ to $3.5\,\mathrm{m\,s^{-1}}$ is imposed. Furthermore, the absolute value of the peak force $F_{\max}$ should be below $50\,\mathrm{kN}$. Regarding damping, closing operation is more critical as the bellows accelerates the armature in this case and is studied as worst-case. As constraints, damping is considered successful if the armature ends in a position within $0.5\,\mathrm{mm}$ from the TC with a velocity below $0.1\,\mathrm{m\,s^{-1}}$. If damping is too weak or too strong, the armature hits the damping TC or does not come close enough to the damping TC. It is possible that the damping force is strong enough to reverse the direction of the armature and to accelerate the armature out of the $0.5\,\mathrm{mm}$ zone. This is referred to as *Reversal* in this work. In the worst-case, *Reversal* could lead to unintentional reopening or reclosing. If the damping force has declined to zero while the armature still is in the $0.5\,\mathrm{mm}$ zone, it is assumed that a bistable mechanism pulls the armature towards the TC and holds it in place.

III. FEM Model

The TCA was modelled in the FEM software Comsol. The electromagnetic equations consisted of the Maxwell equations. The movement of the armature was considered with a moving mesh. The mechanical part was modelled using a lumped-element approach with the following differential equation:

$$m\ddot{d} = -mg + F_\mathrm{L} + F_\mathrm{B}, \quad (1)$$

where $m = 2.2364\,\mathrm{kg}$ is the total moving mass, g the gravitational constant, F_L the Lorentz force, and F_B the force exerted by the bellows. F_L is calculated in the FEM model. The datasheet from the manufacturer of the VI contained a table with F_B as function of d. This was included in the model by making a linear fit in the contact opening range of $10\,\mathrm{mm}$:

$$F_\mathrm{B} = -Ad + B \quad (2)$$

for $d < 0$ with $A = 12.5\,\mathrm{N\,mm^{-1}}$ and $B = 59.17\,\mathrm{N}$. After the current pulse, F_L decays quickly. It is not necessary to simulate the time between the end of the acceleration phase t_0 and the start of the active damping phase t_1. The contact

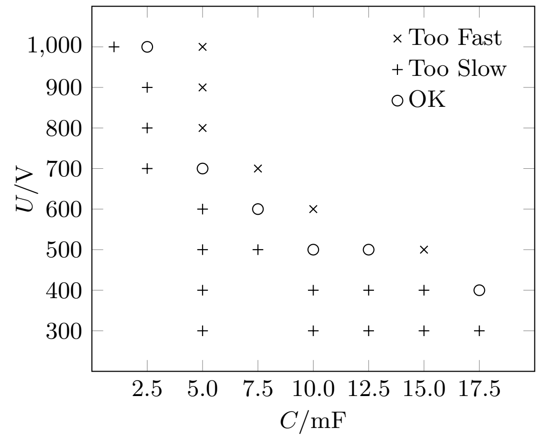

Fig. 5. Evaluation of C and U combinations for Thomson coil opening acceleration phase

distance and armature speed v during this intermediate phase can be calculated from the following equations:

$$d = C_1 \cos \lambda t + C_2 \sin \lambda t + C_3 \quad (3)$$

$$v = -\lambda C_1 \sin \lambda t + \lambda C_2 \cos \lambda t \quad (4)$$

with the coefficients

$$C_1 = (d_0 - C_3) \cos \lambda t_0 - v_0/\lambda \sin \lambda t_0 \quad (5)$$

$$C_2 = (d_0 - C_3) \sin \lambda t_0 + v_0/\lambda \cos \lambda t_0 \quad (6)$$

$$C_3 = (-mg + B)/A \quad (7)$$

and $\lambda = \sqrt{A/m}$. Evaluating (3) and (4) at t_1 yields the initial conditions for the active damping phase.

IV. Simulation Results & Discussion

In order to find suitable values for C and U, simulations have been run for several combinations of both values. In Fig. 5, it is indicated whether the combination led to successful opening or whether the opening speed was too fast or too slow. Note that the force constraint was not violated in any of the simulated cases. It is quite striking that the feasible combinations all correspond to a capacitor energy in the range $1.225\,\mathrm{kJ}$ to $1.563\,\mathrm{kJ}$. However, other aspects may render a combination preferable, for instance the capacitor technology available for the chosen voltage level or the peak force $F_{\max}$. Even if the force constraint is not violated, lower stress may still increase the lifetime of the actuator.

In Fig. 6, $F_{\max}$ is depicted as function of C for the feasible cases from Fig. 5. $F_{\max}$ decreases with increasing C, but it takes longer time to accelerate the armature to peak velocity.

In Fig. 7, different combinations of U and the contact distance at the start of damping d_1 for damping during closing operation are studied. As visible, only few combinations do not violate the constraints. Compared to the results from [5], [6], this may be surprising, but it has to be considered that the moving mass was significantly heavier in this work. The general tendencies are the same as in the above-mentioned studies: Damping becomes more effective if damping is started

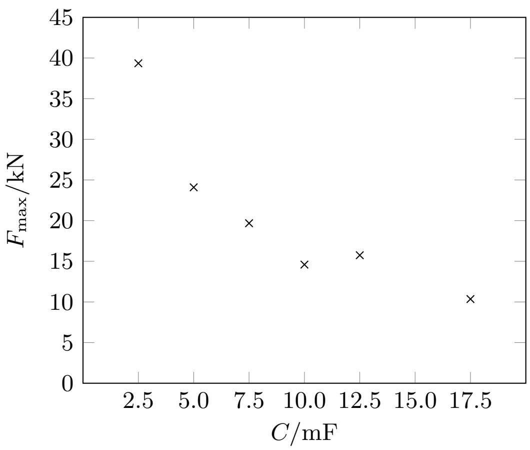

Fig. 6. Peak force during opening acceleration phase as function of C for feasible C and U combinations

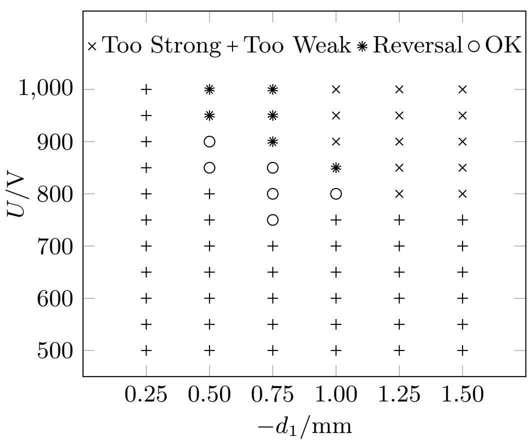

Fig. 7. Evaluation of contact distance at the start of damping and U values for Thomson coil closing damping ($C = 5\,\mathrm{mF}$)

closer to the damping TC. However, if damping is started at $d_1 = -0.25\,\mathrm{mm}$ the damping force is not sufficient to decelerate the armature before it hits the TC. In this work, U has to be higher for damping than for acceleration.

The d-t curve and v-t curve for opening and closing operation are shown in Fig. 8. The opening time is $3.64\,\mathrm{ms}$ and the closing time is $3.36\,\mathrm{ms}$. It may be attempted to apply voltage stress to the VI before the actuation is complete as the VI can endure high lightning impulse voltage up to $95\,\mathrm{kV}$ and rated power frequency withstand voltage up to $42\,\mathrm{kV}$ for $1\,\mathrm{min}$ compared to the normal operation rating of $12\,\mathrm{kV}$.

V. Conclusion

In this work, the system design of a TCA system with active damping for a VI in DCCB applications was described, especially regarding the selection of C and U for the drive circuit. FEM simulation results were provided for opening and closing operation. The results showed that acceptable parameter combinations led to approximately the same stored energy. The chosen C value yields decent opening/closing time

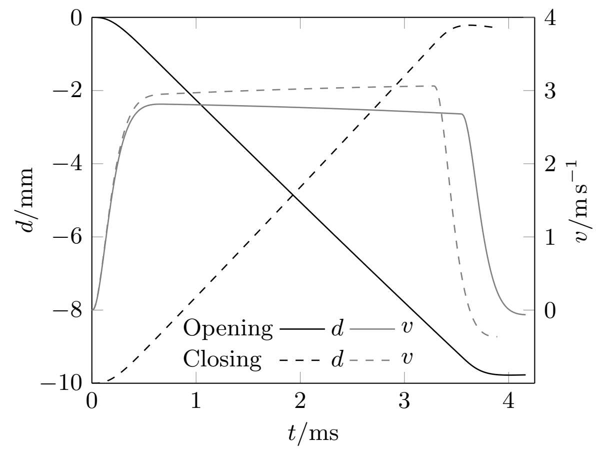

Fig. 8. Contact distance and speed curve for opening and closing operation ($C = 5\,\mathrm{mF}$, $U = 700\,\mathrm{V}$ for acceleration and opening damping, $U = 800\,\mathrm{V}$ for closing damping, damping initiated $0.75\,\mathrm{mm}$ from the respective Thomson coil)

and some range for higher U as active damping requires a higher U than acceleration. The simulation results also showed that the range of U and the instant of active damping are quite narrow for successful damping. The chosen C and U combination led to an opening time of $3.64\,\mathrm{ms}$ and a closing time of $3.36\,\mathrm{ms}$. Challenges that need to be addressed in future work are the power supply of the drive circuit and thermal problems of the TCA during aborted proactive commutation and auto-reclosing operation.

References

[1] C. M. Franck, "HVDC Circuit Breakers: A Review Identifying Future Research Needs," *IEEE Transactions on Power Delivery*, vol. 26, no. 2, pp. 998–1007, Apr. 2011.

[2] T. Augustin, S. Norrga, and H.-P. Nee, "Modelling of HVDC breakers for HVDC grid simulations," in *13th IET International Conference on AC and DC Power Transmission*, Manchester, Feb. 2017, pp. 1–6.

[3] S. Tokoyoda, T. Inagaki, F. Page, M. Sato, K. Kamei, M. Miyashita, and H. Ito, "Interruption characteristics of vacuum circuit breaker and the application to DCCB," in *13th IET International Conference on AC and DC Power Transmission*, Manchester, Feb. 2017, pp. 1–5.

[4] A. Bissal, "Modeling and Verification of Ultra-Fast Electro-Mechanical Actuators for HVDC Breakers," Ph.D. dissertation, KTH Royal Institute of Technology, Stockholm, 2015.

[5] G. Engdahl, J. Magnusson, A. Bissal, and M. Sparr, "An Exploratory Study of the Retardation Ability of a Thomson Coil Actuator," in *15th International Conference on New Actuators*, Bremen, Jun. 2016, pp. 1–4.

[6] C. Peng, L. Mackey, I. Husain, A. Huang, W. Yu, B. Lequesne, and R. Briggs, "Active Damping of Ultrafast Mechanical Switches for Hybrid AC and DC Circuit Breakers," *IEEE Transactions on Industry Applications*, vol. 53, no. 6, pp. 5354 – 5364, Aug. 2017.

[7] T. Augustin, M. Becerra, and H. P. Nee, "Advanced Test Circuit for DC Circuit Breakers," in *20th European Conference on Power Electronics and Applications (EPE'18 ECCE Europe)*, Riga, Sep. 2018, pp. 1–8.

[8] Z. Chen, Z. Yu, X. Zhang, T. Wei, G. Lyu, L. Qu, Y. Huang, and R. Zeng, "Analysis and Experiments for IGBT, IEGT, and IGCT in Hybrid DC Circuit Breaker," *IEEE Transactions on Industrial Electronics*, vol. 65, no. 4, pp. 2883–2892, Apr. 2018.

[9] W. Wen, Y. Huang, T. Cheng, S. Gao, Z. Chen, X. Zhang, Z. Yu, R. Zeng, and W. Liu, "Research on a current commutation drive circuit for hybrid dc circuit breaker and its optimisation design," *IET Generation, Transmission Distribution*, vol. 10, no. 13, pp. 3119–3126, Oct. 2016.

E-mail of the author: timau@kth.se